Spin Wave Wells in Nonellipsoidal Micrometer Size Magnetic Elements

J. Jorzick, S. O. Demokritov,* and B. Hillebrands

Fachbereich Physik, Universität Kaiserslautern, 67663 Kaiserslautern, Germany

M. Bailleul and C. Fermon

Service de Physique de l'Etat Condens, CEA Saclay, Gif sur Yvette, France

K. Y. Guslienko[1] and A. N. Slavin[2]

[1]*Seagate Research, 2403 Sidney Street, Pittsburgh, Pennsylvania 15203*
[2]*Department of Physics, Oakland University, Rochester, Michigan 48309*

D. V. Berkov and N. L. Gorn

Innovent Jena, Jena, Germany

We show experimentally and by model calculations that in finite, nonellipsoidal, micrometer size magnetic thin film elements the dynamic magnetic eigenexcitations (spin waves) may exhibit strong spatial localization. This localization is due to the formation of a potential well for spin waves in the highly inhomogeneous internal magnetic field within the element.

            PACS numbers: 75.30.Ds, 75.40.Gb

Recently the fabrication and study of laterally patterned magnetic structures from micrometer to nanometer sizes became possible attracting large interest due to applications in the fields of high density magnetic storage [1]. From the point of view of fundamental studies, the reduction of dimensionality brings into play confinement phenomena that affect the dynamic properties of the system to a large extent [2]. An understanding of these new phenomena is also highly demanded for high data rate applications.

Spin waves, as the fundamental dynamic eigenmodes of a magnetic system, define the time scale of a magnetization reversal process. The problem of spin waves in an ellipsoidal element is straightforward, since the internal magnetic field in this case is homogeneous [3,4]. On the other hand, it is known that in a nonellipsoidal element the internal field decreases near the edges of the element [5]. In some cases zones with zero internal fields can be created [6].

In this Letter we report on the study of dynamic excitations in nonellipsoidal magnetic elements (long stripes and rectangular elements) with a large inhomogeneity of the internal field. We report the observation of a novel, strongly spatially localized spin wave mode. This mode appears near those edges of the element that are perpendicular to the applied magnetic field. The spatial localization takes place due to the high inhomogeneity of the internal field in these regions, which creates a potential well for the spin waves.

The investigated samples were prepared from $d = 30-35$ nm thick permalloy ($Ni_{80}Fe_{20}$) films, thermally evaporated on Si(111) substrates in UHV. Patterning was performed by means of e-beam lithography. The rectangular elements have lateral dimensions of $1 \times (1-2)$ μm^2 and the spacing $\delta = 0.1-1$ μm between the elements. Stripes with a width of $w = 1$ μm, a length of 90 μm, and a distance between the stripes of 0.5 μm were prepared. The elements were arranged in arrays of dimensions of 500×500 μm^2. The high quality of the patterning process has been confirmed by scanning force microscopy.

Thermally excited spin waves were investigated by using a Brillouin light scattering (BLS) in backscattering geometry [7]. In all experiments both the magnetic field and the wave vector $\mathbf{Q}$ transferred in the light scattering process lie in the plane of the elements. The wave vector was oriented perpendicular to the stripe axes or along one of the edges of the elements. The absolute value of $\mathbf{Q}$ was varied in the range of $Q = (0-2.5) \times 10^5$ cm^{-1}. An external magnetic field $\mathbf{H}_e$ was applied in the plane of the elements. Contrary to our earlier studies on spin wave quantization [8,9], where the stripes were magnetized along their long axes, different in-plane orientations of $\mathbf{H}_e$ were studied in the present work.

It has recently been shown [9,10] that the intensity of light inelastically scattered from laterally confined spin wave modes for a given Q is proportional to the Fourier component of the mode profile squared, m_Q^2. Thus, by measuring the BLS intensity as a function of Q one can derive the spatial profile of $m(r)$. The interval in Q, in which a significant BLS intensity is observed, is inversely proportional to the confinement width of the mode in the real space, Δr: $\Delta Q \approx 2\pi/\Delta r$.

In the following we assume a Cartesian coordinate system in which the x axis is perpendicular to the plane of the elements, and the y axis is along the long axes of the stripes. Figure 1 shows two typical BLS spectra obtained from an array of stripes for the external in-plane magnetic field $H_e = 500$ Oe for different orientations of the field.
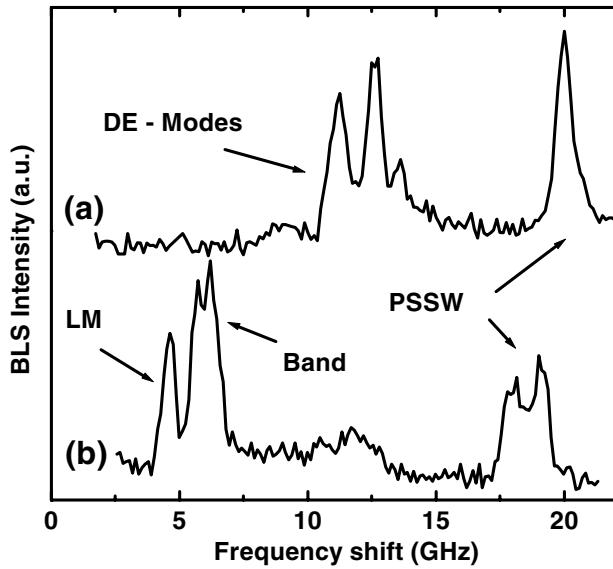
FIG. 1. BLS spectra obtained on the stripe array for $Q = 1 \times 10^5$ cm^{-1} at $H_e = 500$ Oe for (a) the DE geometry and (b) the BWVMS geometry. LM indicates the localized mode.

Spectrum 1(a) is obtained for $\mathbf{H}_e$ oriented along the y axis, thus presenting the so-called Damon-Eshbach (DE) geometry [11] investigated in detail in our previous works [8,9]. Spectrum 1(b) is recorded with both $\mathbf{Q}$ and $\mathbf{H}_e$ aligned along the z axis. As it is seen in Fig. 1, both spectra contain several distinct peaks corresponding to spin wave modes. The high frequency peaks can easily be identified as exchange dominated perpendicular standing spin wave (PSSW) modes, and they are also observed in unpatterned films. Their frequencies are determined by the exchange interaction and the internal field. To investigate the nature of the other observed excitations, the dispersion was measured by varying Q. It is displayed in Fig. 2 for both orientations of $\mathbf{H}_e$.
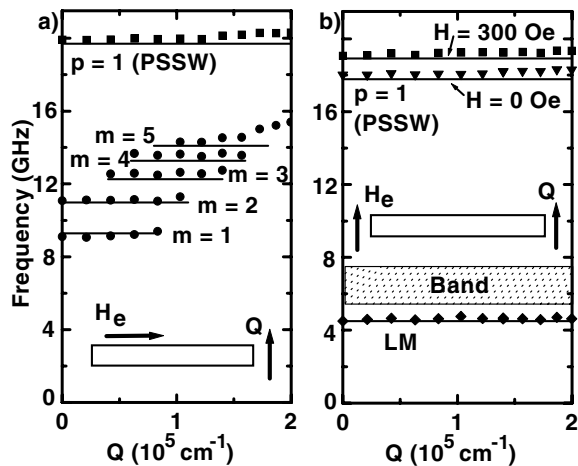

FIG. 2. Spin wave dispersion of the stripe array measured at $H_e = 500$ Oe for (a) the DE geometry and (b) the BWVMS geometry. The solid lines represent the results of calculation.

Figure 2a representing the DE geometry clearly demonstrates the lateral quantization of the DE spin waves, resembling a typical "staircase" dispersion [8,9]. The interval of the observation of each mode in the Q space $\Delta Q \approx (0.8-1.0) \times 10^5$ cm^{-1} is in agreement with the width of the stripe $w = 1$ μm, giving $2\pi/w = 0.63 \times 10^5$ cm^{-1}. The frequency of the PSSW mode coincides with that of the PSSW mode for the unpatterned film and corresponds to an internal field of $H = H_e = 500$ Oe thus corroborating negligible demagnetizing effects in the stripes magnetized along their long axes.

The dispersion presented in Fig. 2b for $\mathbf{H}_e$ parallel to the z axis [i.e., $\mathbf{H}_e \| \mathbf{Q}$, so-called backward volume magnetostatic spin wave (BWVMS) geometry] differs completely from that shown in Fig. 2a. First, the PSSW mode is split into two modes, with frequencies corresponding to internal fields of $H = 300$ Oe and $H = 0$ Oe, respectively. This corroborates the well-known fact that the internal field is determined by essential demagnetizing effects and can be zero near the stripe edges [6]. Second, a broad peak is seen in the spectra in the frequency range 5.5–7.5 GHz over the entire accessible interval of Q. The shape of the peak varies with Q, thus indicating different contributions of unresolved modes to the scattering cross section at different Q. Third, a separate, low frequency, dispersionless mode with a frequency near 4.6 GHz (indicated as "LM" in Figs. 1 and 2) is observed over the entire accessible wave vector range ($q_{max} = 2.5 \times 10^5$ cm^{-1}) with almost constant intensity. This is a direct confirmation of a strong lateral localization of the mode within a region with the width $\Delta r < 2\pi/q_{max} = 0.25$ μm. From the low frequency of the mode one can conclude that it is localized near the edges of the elements, since these are the field-free regions [5,6].

Further evidence is provided by the observation of a corresponding mode in rectangular elements (not shown). For example, the frequency of the lowest mode for the rectangular elements with the lateral sizes 1×1.75 μm^2, the distance between the elements $\delta = 0.2$ μm, and the thickness $d = 33$ nm is 5.3 GHz.

A quantitative analytical description of the spin wave modes observed in the stripes is made as follows. The frequency ν of the spin wave is then given by

$$\nu(q) = \frac{\gamma}{2\pi}\left[\left(H + \frac{2A}{M_S}q^2\right) \right.$$
$$\left. \times \left(H + \frac{2A}{M_S}q^2 + 4\pi M_S \cdot F_{pp}(Qd)\right)\right]^{1/2},$$
(1)

where H is the internal static magnetic field, M_S the magnetization, A the exchange constant, and $F_{pp}(Qd)$ the matrix element of dipole-dipole interaction [12]. The spin-wave wave vector $\mathbf{q} = q_p\mathbf{e}_x + \mathbf{Q}$ consists of the perpendicular part $q_p = p\pi/d$ quantized due to the finite film thickness, and the in-plane part $\mathbf{Q} = Q_y\mathbf{e}_y + Q_z\mathbf{z}$.

If, for reference, $\mathbf{H}_e \parallel \mathbf{e}_y$ and $\mathbf{Q} \parallel \mathbf{e}_z$ (the DE geometry), the analysis of spin wave quantization is straightforward [9]. One assumes a quantization condition for Q: $Q = m\pi/w$ where $m = 1, 2, 3 \ldots$. The frequencies of these quantized modes calculated using Eq. (1) for $p = 0$, $m = 1, 2, 3, 4, 5$ (laterally quantized modes) and for $p = 1$ and $m = 0$ (PSSW) are in good quantitative agreement with the results of the experiments as shown in Fig. 2a. The material parameters used are $4\pi M_S = 10.2$ kOe, $A = 10^{-6}$ erg/cm^2, and $\gamma/2\pi = 2.95$ GHz/kOe.

If $\mathbf{H}_e \parallel \mathbf{e}_z$, the effect of demagnetization due to the finite wire width is very large, and the internal magnetic field is strongly inhomogeneous and differs from H_e. It can be evaluated as [5,6]

$$H(x, y, z) = H_e - N_{zz}(x, y, z) \cdot 4\pi M_S, \qquad (2)$$

where $N_{zz}(x, y, z)$ is the demagnetizing factor. As it will be discussed below, this inhomogeneous field creates a potential well for spin waves resulting in localization. The averaged value of $H(z)$ obtained by integrating Eq. (2) along the axes x and y over the stripe cross section is shown in the inset of Fig. 3. For $H > 0$ the magnetization is parallel to $\mathbf{H}_e$. Near the edges, however, regions with $H = 0$ and with continuously rotating magnetization are formed [6]. Since the rotation of the static magnetization dramatically changes the dispersion of spin waves [11], regions with zero internal field reflect spin waves propagating from the middle of the stripe towards these regions. On the other hand, a spin wave propagating in an inhomogeneous field might encounter the second turning point even if the magnetization is uniform. In fact, for large enough values of the internal field there are no allowed real values of Q, consistent with the spin wave dispersion [13]. Thus, a potential well for propagating spin waves is created. Similar to the potential well in quantum mechanics, the conditions determining the frequencies ν_n of possible spin wave states in the well created by the inhomogeneous internal field are determined by the equation

$$\int Q[H(z), \nu] \, dz = r\pi, \qquad (3)$$

where $r = 1, 2, 3, \ldots$. and $Q[H(z), \nu]$ is found from the spin wave dispersion.

We will illustrate these ideas in the following. The dispersion curves for spin waves with $\mathbf{Q} \parallel \mathbf{H}$ and $p = 0$ calculated using Eq. (1) for different constant values of the field are presented in Fig. 3. A dashed horizontal line shows the frequency of the lowest spin wave mode $\nu_1 = 4.5$ GHz obtained from Eq. (3) for $r = 1$ in good agreement with the experiment. It can be seen from Fig. 3 that for $H > 237$ Oe there are no spin waves with the frequency $\nu_1 = 4.5$ GHz. Therefore, the lowest mode can exist only in the spatial regions in the magnetic stripe
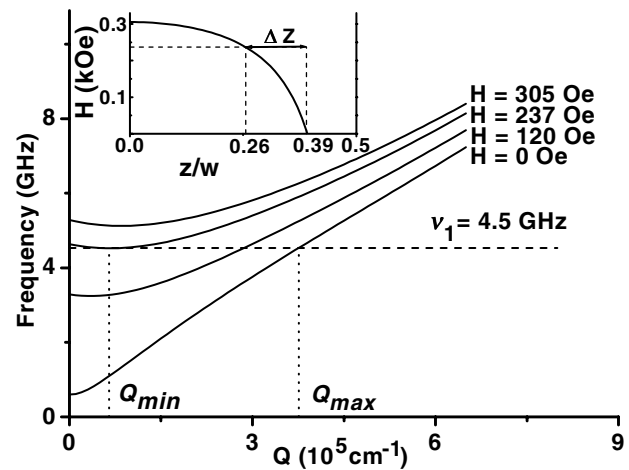

FIG. 3. Dispersion of plane spin waves in the BWVMS geometry at constant internal fields as indicated. Inset: the profile of the internal field in a stripe. Δz shows the region of the lowest mode localization.

where 0 Oe $< H < 237$ Oe. The corresponding turning points are indicated in the inset of Fig. 3 by the vertical dashed lines. Thus, the lowest mode is localized in the narrow region Δz near the lateral edges of the stripe where $0.26 < |z/w| < 0.39$. The mode is composed of exchange dominated plane waves with $Q_{min} < Q < Q_{max}$, as indicated in Fig. 3.

The higher order spin wave modes with $r > 1$ having their frequencies above 5.3 GHz are not strongly localized and exist anywhere in the stripe where the internal field is positive ($0 < |z/w| < 0.39$). In the experiment they show a band, since the frequency difference between the ν_r and ν_{r+1} modes is below the frequency resolution of the BLS technique.

The one-dimensional analytical approach presented above is applicable to long magnetic stripes. To describe the spin wave modes of two-dimensional rectangular elements, shown in Fig. 4a, we performed micromagnetic simulations of nonuniform magnetic excitations in such elements. The method used is based on the Langevin dynamics, and the time evolution of the magnetization distribution in the magnetic element, which is discretized into $N_x \times N_z = 100 \times 180$ cells with magnetic moments $\boldsymbol{\mu}_i$, is simulated using the stochastic Landau-Lifshitz-Gilbert (LLG) equation [14]. The effective field $\mathbf{H}_i^{\text{eff}}$ acting on the ith moment consists of a deterministic part $\mathbf{H}_i^{\text{det}}$ (which includes external magnetic field and the fields created by the exchange and dipolar interactions between different cell moments) and a fluctuating part $\mathbf{H}_i^{\text{fl}}(t)$. The correlation properties of this fluctuating field, which is intended to simulate the influence of thermal fluctuations, may be quite complicated in our micromagnetic system with interaction in contrast to the standard single-particle situation [15]. These properties are not studied so far. It is, however, a common practice, to use a simple approximation describing the fluctuating field in the form
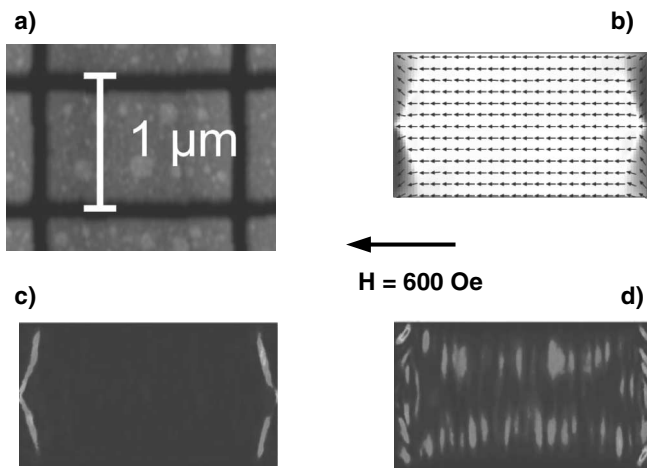
FIG. 4. (a) AFM image of rectangular elements; (b) calculated distribution of static magnetization in an element; (c) mode profile of a low-frequency spin wave mode with $\nu = 5.3$ GHz (note the mode localization near the edges); (d) mode profile of a spin wave mode with $\nu = 12.2$ GHz.

of the δ-correlated random noise [14,16,17]. We believe that the results of simulations with such a delta-correlated noise should provide at least qualitatively a correct picture of spatial distribution of different magnetic eigenmodes in the system. In frame of this approximation the noise power has been calculated for a system of interacting magnetic cells as in [16]. The stochastic LLG equation has then been solved using the modified Bulirsch-Stoer method (details of the method will be given elsewhere [18]).

The starting state (Fig. 4b) for the simulation was obtained by solving the LLG equation without any fluctuations. Next the field $\mathbf{H}_i^{\mathrm{fl}}(t)$ has been turned on. After the thermodynamic equilibrium state of the system has been reached, the obtained values of all cell moments were recorded. Afterwards, using Fourier analysis, the oscillation spectrum of the total magnetic moment of the element was obtained. In the frequency interval 3–20 GHz this Fourier spectrum demonstrates several maxima. The Fourier components of *each* cell magnetization $\boldsymbol{\mu}_{i,\omega}$ corresponding to these maxima were calculated and squared, to compare them with the measured spin wave intensities. As an example, the obtained spatial distributions for the frequencies $\nu = 5.3$ GHz and $\nu = 12.2$ GHz are presented in Figs. 4c and 4d. It is clear from Fig. 4c that the low-frequency mode is strongly localized in the narrow regions near the edges of the elements that are perpendicular to the applied field. In contrast, and for comparison, the mode with $\nu = 12.2$ GHz shown in Fig. 4d is not localized.

In conclusion, we have demonstrated the eigenmode spectrum of magnetic stripes and rectangular elements. In particular, we have shown the existence of a new, spatially localized spin wave mode of exchange nature in finite magnetic elements with the localization caused by the inhomogeneity of the internal field. These modes must be taken into account for yielding a better understanding of, e.g., the fast magnetic switching properties in magnetic memory elements.

*Email address: demokrit@physik.uni-kl.de.

[1] For example, *The Physics of Ultrahigh-Density Magnetic Recording,* edited by M. Plumer, J. van Ek, and D. Weller (Springer, Berlin, 2001).
[2] S. O. Demokritov, B. Hillebrands, and A. N. Slavin, Phys. Rep. **348**, 441 (2001).
[3] C. Kittel, Phys. Rev. **73**, 155 (1948).
[4] L. R. Walker, Phys. Rev. **105**, 390 (1957).
[5] R. I. Joseph and E. Schlömann, J. Appl. Phys. **36**, 1579 (1965).
[6] P. Bryant and H. Suhl, Appl. Phys. Lett. **54**, 2224 (1989).
[7] B. Hillebrands, Rev. Sci. Instrum. **70**, 1589 (1999).
[8] C. Mathieu, J. Jorzick, A. Frank, S. O. Demokritov, A. N. Slavin, B. Hillebrands, B. Bartenlian, C. Chappert, D. Decanini, F. Rousseaux, and E. Cambrill, Phys. Rev. Lett. **81**, 3968 (1998).
[9] J. Jorzick, S. O. Demokritov, C. Mathieu, B. Hillebrands, B. Bartenlian, C. Chappert, F. Rousseaux, and A. N. Slavin, Phys. Rev. B **60**, 15 194 (1999).
[10] J. F. Cochran, J. Magn. Magn. Mater. **212**, 40 (2000).
[11] R. W. Damon and J. R. Eshbach, J. Phys. Chem. Solids **19**, 308 (1961).
[12] B. A. Kalinikos and A. N. Slavin, J. Phys. C **19**, 7013 (1986).
[13] E. Schlomann and R. I. Joseph, J. Appl. Phys. **35**, 167 (1964).
[14] J. L. Garcia-Palacios and F. J. Lazaro, Phys. Rev. B **58**, 14 937 (1998).
[15] W. F. Brown, Jr., Phys. Rev. **130**, 1677 (1963).
[16] H.-B. Braun, in *Structure and Dynamics of Heterogeneous Systems,* edited by P. Entel and D. Wolf (World Scientific, Singapore, 2000).
[17] G. Brown, M. A. Novotny, and P. A. Rikvold, Phys. Rev. B **64**, 134422 (2001).
[18] D. V. Berkov and N. L. Gorn (to be published).